Carbon-coated silver nanoparticles dispersed in a 2024 aluminum alloy produced by mechanical milling

C. Carreño-Gallardo, I. Estrada-Guel, M.A. Neri a, E. Rocha-Rangel, M. Romero-Romo, C. López-Meléndez, **R. Martínez-Sánchez.**

Abstract

Aluminum-based nanocomposites were produced by dispersing different contents of carbon-coated silver nanoparticles (Ag-C NP) into a 2024 aluminum alloy (Al_{2024}). After milling nanostructures about 100 nm grain sizes were obtained. Increment in mechanical properties was observed in all composites synthesized. The reinforcement nanoparticles were distributed homogeneously into the Al_{2024} matrix by mechanical milling process. The yield strength (σ_y) and Brinell hardness (HB), of the nanocomposites increased as the nanoparticles content was increased as well.

1. Introduction

Discontinuously reinforced metal matrix composites have received much attention for both academics and manufacturing industries in recent years, primarily to meet the demand for lower weight and higher strength; it has been used for applications in aerospace, naval and automotive structures [1]. Considerable progress in the field of composite materials has been made, driven by the relentless need for advanced materials with improved performance. Many recent studies have employed powder metallurgy (P/M) in the fabrication of Al alloy because the fabrication of the net-shaped part can be achieved at a low cost [2,3]. Wide varieties

of particulates and fibers have been used as reinforcement. Recently, a considerable amount of research in novel nanocomposites synthesis has been directed towards using nano-sized reinforcing materials [4].

The idea behind strength enhancement in dispersion-strengthened materials lies in the introduction of a high strength dispersed phase into the matrix. This phase can be introduced into the matrix from outside, or it can be formed “in situ” during the milling.

A method to improve particle distribution is to use mechanical alloying technique or mechanical milling (MM) process [5–8].

In this work, mechanical milling was used to produce a nanocomposite by dispersing carbon-coated silver nanoparticles into commercial 2024 aluminum alloy. Mechanical properties were evaluated as a function of carbon-coated silver nanoparticles content. The microstructure of the composites was evaluated by scanning electron microscopy (SEM) and transmission electron microscopy (TEM).

2. Experimental procedure

The raw material used in this study was 2024 commercial aluminum alloy (Al_{2024}). The Ag-C NP is a product obtained from Nanotechnologies, Inc. (Austin, TX), which is produced by arc discharge and stabilized with carbon from a hydrocarbon source. These particles are stable and easy to handle. As the nanometric carbon layers are attached to the silver particles they are not dissolved into Al matrix, and can be easily dispersed in it. The chemical composition of Al_{2024} and carbon-coated silver nanoparticles (Ag-C NP) is shown in Table 1. The Al_{2024}powder was produced by machining a solid extruded bar. The machined metal

shavings were mixed with Ag-C NP in different concentrations (0.00, 0.50, 1.00, 1.50, 2.00, 2.50 wt.% Ag-C NP), and were mechanically milled in a high-energy horizontal attritor mill (ZOZ CM01 Simoloyer); container and milling media were made from hardened steel. A ball to powder (metal shavings) weight ratio of 20:1 was used in all runs. In order to avoid excessive welding of the powders, 10 drops of methanol were added to the powder mixtures, previous to milling runs. Argon flux was used as the milling atmosphere and the milling time was set to 10 h.

The as-milled products were cold compacted under a uniaxial pressure of ~60 tons, followed by pressureless sintering at 773 K during 2 h under vacuum (~1 Torr). Sintered samples were held 30 min at 773 K and then hot

Table 1
Composition of the Al_{2024} used (wt.%) in this work.

Al	90.7–94.7
Cr	Max. 0.1
Cu	3.8–4.9
Fe	Max. 0.5
Mg	1.2–1.8
Mn	0.3–0.9
Si	Max. 0.05
Ti	Max. 0.15
Zn	Max. 0.25

extruded into a 10 mm diameter rod; an extrusion ratio of 16 was used for all composites.

Morphology characterization was carried out by a scanning electron microscope JEOL-SM 5800 operated at 20 kV. Microstructural characterization was carried out through X-ray diffraction in a Siemens diffractometer with Cu Kα radiation (λ = 1.5406 Å) and operated at 40 kV and 25 Amp in the 2θ range of 30–100°. The step and acquisition time were 0.05° and 5 s, respectively. Structural analysis was carried out by TEM in a Philips CM 200 operated at 200 kV. Chemical analysis was

carried out by characteristic X-ray energy dispersion spectroscopy (EDS) with a DX4 X-ray energy dispersive spectrometer coupled with a transmission electron microscope. Hardness of the extruded samples was determined with a Wilson/Rockwell INSTRON, using a 1/16 indentation ball and a maximum load of 100 kgf. Later the Rockwell values were converted to Brinell scale. The average values of eight points of randomly selected regions in each sample are reported in this study.

The tensile tests were carried out wit INSTRON testing equipment at room temperature and at constant displacement rate of 2 mm/min. The yield strength was measured at the elastic limit and maximum stress was determined from a tensile strength vs. strain plot.

3. Results and discussion

3.1. As-milled products

Fig. 1 shows the XRD spectra of all composites studied in the present work after 10 h of milling. Al_{2024} not milled was included as reference sample. By comparing the spectra from reference sample with those obtained from composites (different contents of Ag-C NP), no appreciable differences were found; this probably was because the small amount of Ag-C NP added to Al_{2024} alloy. The diffraction patterns show a small broadening of Al peaks after milling, which may be a result of the deformation induced by the processing and the refining of the microstructure. No signals from silver or graphite were observed, which is due to the nanometric size of Ag-C NP. Fig. 2 shows a TEM bright field image of the as-milled Al2024–1 wt.% Ag-C NP sample. Fig. 2 shows conventional TEM images of the Al sample with 1% of

Ag-C NP. The contrast corresponds to bend contours, grain boundaries and dislocations.

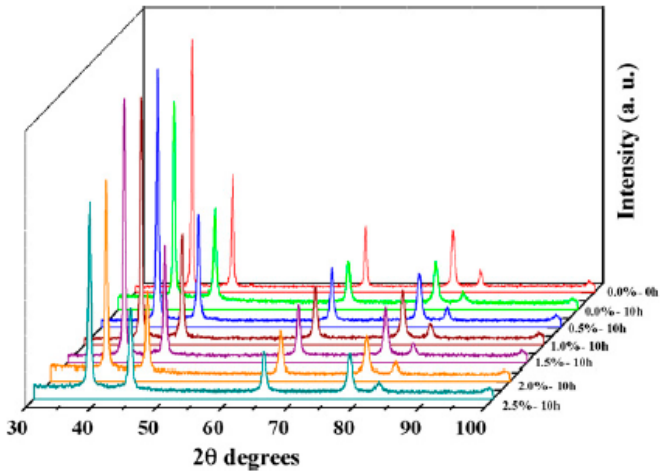

Fig. 1. XRD spectra from as-milled composites as a function of Ag-C NP content. Reference sample (0.0%, 0 h) is included for comparison. Notice the similar shape in all spectra.

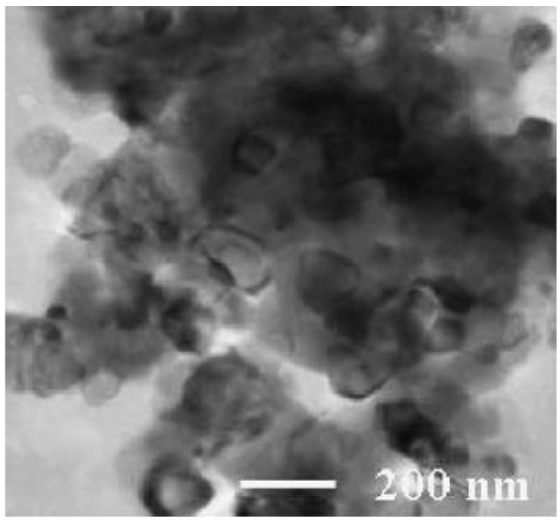

Fig. 2. TEM bright field image of the as-milled Al2024–1 wt.% Ag-C NP composite sample. Dark spot correspond to silver nanoparticles.

The grain size of the Al-based matrix is the range 30–200 nm. All composites showed equiaxial grains. The dispersed Ag-C NP particles (dark spots) have of about 20 nm in size and are homogeneously dispersed in the matrix.

3.2. Consolidated products

Fig. 3 shows a XRD spectrum from Al-based composite with 1% of Ag-C NP in the as-milled and as-extruded conditions. Sharp peaks are observed in sample identified as “extruded”, indicating a grain growth in the composites after sintering and hot extrusion processes. However the most important aspect was the precipitation of the tetragonal body centered Al2Cu phase (ICDD card no. 25-0012) during sintering-extrusion sequence. During the thermo-mechanical treatments this phase was crystallized from the aluminum solid solution formed during the mechanical milling process. Because of the low cooling rates used during the sintering and hot extrusion process, this phase crystallized after the normalized temper condition.

Presence of Al2Cu was corroborated by SEM analyses (Fig. 4). Fig. 4a shows a representative view of the microstructure of the Al-based composites. This figure shows an aluminum

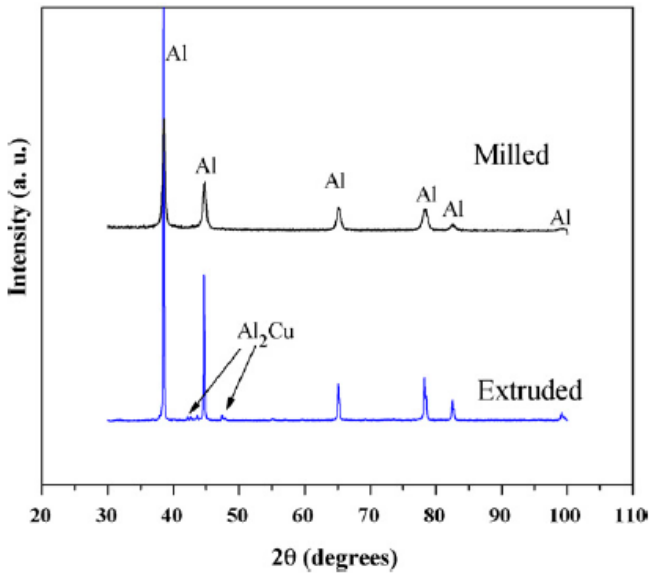

Fig. 3. XRD spectrum from Al_{2024}–1 wt.% Ag-C NP composite sample (as-extruded and milled condition).

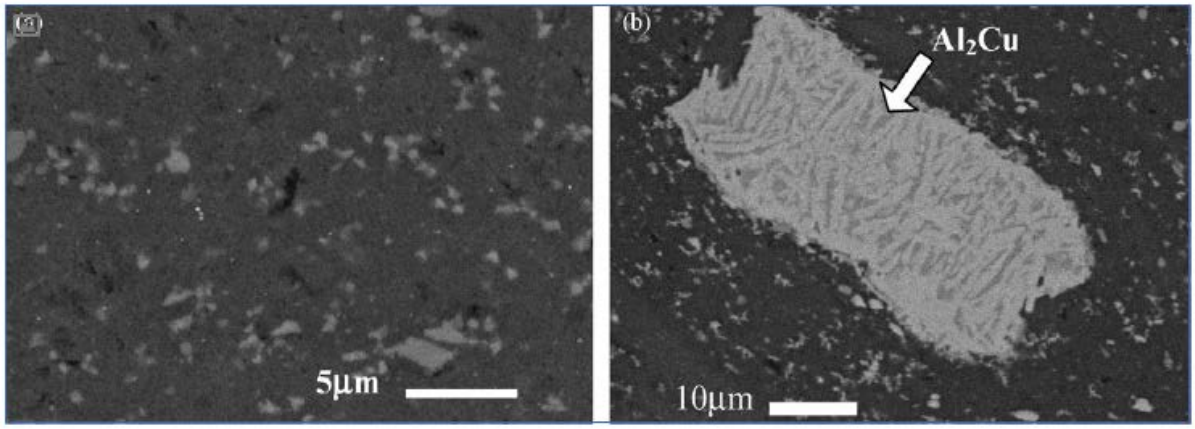

Fig. 4. SEM micrographs from Al_{2024}–1 wt.% Ag-C NP composite sample, showing the presence of Al_2Cu phase.

matrix (dark phase) and bright spots corresponding to Al–Cu phase. Fig. 4b shows a bright particle at higher magnification, EDS results shown that this particle have an Al:Cu ratio of ~2:1 (at.%); which correspond to the stoichiometry of the phase Al2Cu.

Fig. 5 shows the Brinell hardness of the different composites in the as-extruded condition as a function of the Ag-C NP content. The increase of hardness as a function of the reinforcement content is due to both work hardening (mechanical milling) and dispersion hardening. These values are significantly higher than the one referred in the literature for Al2024 alloy in the annealed condition (35 HB).

The increase in composite hardness as a function of the addition of nanoparticles is also important. From 0.0 to 2.5 wt.% of Ag-C NP the increase is on the order of 30 Brinell units. It has been reported that stronger matrix alloys tend to produce stronger composites although the increase in strength due to the reinforcement tends to be lower when higher strength matrix alloys are used. In the case of lower strength matrix alloys, the strengthening effect due to the reinforcement is higher [10]. Even though the 2024 aluminum alloy is considered

strong alloy, and a low level of reinforcement by dispersion is expected, 30 units on the Brinell scale is more than the hardness of pure aluminum (~23 HB) and several aluminum alloys [9].

Fig. 6 shows the yield strength (σy) variation as a function of Ag-C NP content. All samples followed a milling–sintering–hot extrusion sequence. All samples were tested in the extrusion direction. An important effect of Ag-C NP content on the mechanical

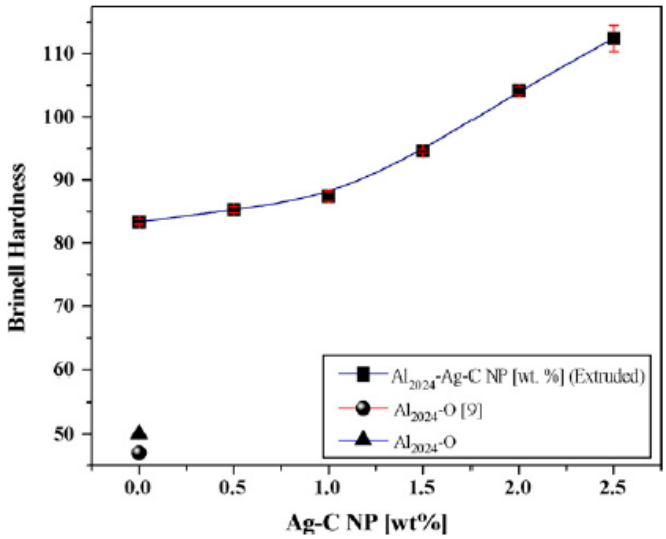

Fig. 5. Brinell hardness as a function of Ag-C NP content for as-extruded compos-
ites. (▲) Corresponds to hardness value of the annealed Al2024 alloy. (●) Data from matweb [9] for 2024 aluminum alloy in annealing condition.

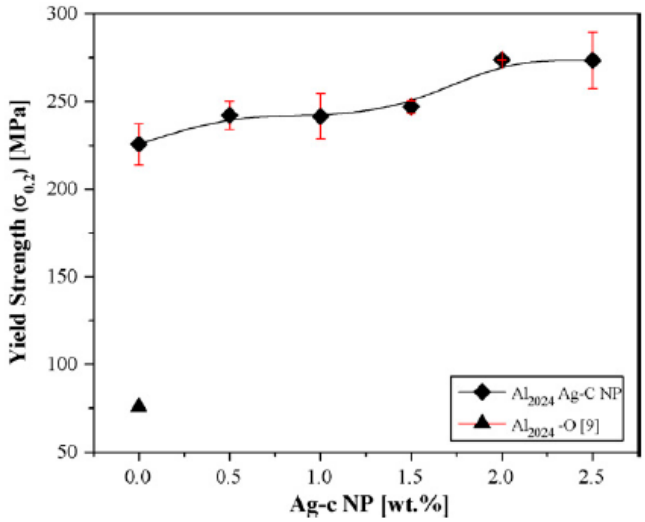

Fig. 6. σ_y as a function of Ag-C NP content. (▲) Data from matweb [9] for 2024 aluminum alloy in annealing condition.

properties was observed. σy shows a positive slope as a function of Ag-C NP content. σy increased from 225.73 to 277.38 MPa which correspond to an increment of about 22.8%. However, the most important aspect is the high values obtained when compared with data reported in literature [9]. The values obtained for the composites in the hot extruded condition (which could be very similar to annealed condition) are ~300% higher for lower Ag-C NP content, and ~366% higher for 2.5 wt.% content than those reported for an 2024 aluminum alloy in annealed condition [9].

Table 2 shows the data obtained by mechanical evaluations (hardness and tensile test). Some data [9] are included for 2024 alloys with different tempers. Although these values are higher than the ones obtained in our extruded composites, there exists the possibility of obtained better results in our composites, after applying similar thermal treatments (T4, T6 or T86) to our materials.

Table 2
Mechanical properties of Al_{2024}–Ag-C NP composites in as-extruded condition.

Material	σ_0 (MPa)	Brinell hardness
Al-2024–0.0%Ag-C NP	225.7	83.3
Al-2024–0.5%Ag-C NP	242.1	85.2
Al-2024–1.0%Ag-C NP	241.5	87.4
Al-2024–1.5%Ag-C NP	246.9	94.5
Al-2024–2.0%Ag-C NP	273.8	104.1
Al-2024–2.5%Ag-C NP	277.3	112.4
Al-2024-O [9]	75.8	47
Aluminum 2024-T4	324	120
Aluminum 2024-T6	345	125
Aluminum 2024-T86	440	135

4. Conclusions

An Al_{2024}-based composite with different concentrations of Ag-C NP particles as reinforcement was produced by mechanical milling process with a milling time of 10 h. Extruded composite materials show an excellent distribution of Ag-C NP on the aluminum alloy matrix. The microstructure plays an important role in mechanical properties in order to have a good distribution of reinforced particle and Al_2Cu phase along the extruded bar. The hardness and yield strength of the consolidate materials increased as a function of the Ag-C NP content σ_y increased from 225.7 to 277.3 MPa.

Acknowledgements

This work was supported by CONACYT (Y46618). Unites States of America, Air Force Office of Scientific Research, Latin America Initiative, Dr. Jaimie Tiley, Contract No. FA 9550/06/1/0524. Thanks to W. Antunez-Florez, G. Vazquez-Olvera, and E. Torres-Moye for their technical assistance.

References

[1] C. Ümit, Ö. KazimCompos. Sci. Technol., 62 (2002), pp. 275-282

[2] F.V. BeaumontInt. J. Powder Metall., 36 (2000), p. 41

[3] C. Lall, W. HeathInt. J. Powder Metall., 36 (2000), p. 45

[4] T. Laha, Y. Liu, A. AgarwalNanosci. Nanotechnol., 7 (2007), pp. 515-524

[5] Y.B. Liu, J.K.M. Kwok, S.C. Lim, L. Lu, M.O. LaiJ. Mater. Proc. Technol., 37 (1993), pp. 441-451

[6] L. Lu, M.O. Lai, C.W. NgMater. Sci. Eng. A, 252 (2) (1998), pp. 203-211

[7] R. Sankar, P. SinghMater. Lett., 36 (1998), pp. 201-205

[8] F.H. FroesF.H. Froes, J.J. deBarbadillo (Eds.), Proceedings of an ASM International Conference on Structural Applications of Mechanical Alloying, Myrtle Beach, SC, March 27–29, ASM International, Materials Park, OH (1990), pp. 1-14

[9] MatWeb, Online Materials Property Data Sheet, 2008, http://www.matweb.com.

[10] R.T. Dasgupta, H. MeenaiMater. Charact., 54 (2005), pp. 438-445